VOL. 9, NO. 6, JUNE 2014 ISSN 1819-6608
ARPN Journal of Engineering and Applied Sciences


www.arpnjournals.com

PRESSURE AND PRESSURE DERIVATIVE ANALYSIS FOR A VERTICAL WELL IN WEDGED AND T-SHAPED RESERVOIRS

Freddy Humberto Escobar, María Paula Polanco and Wilson Benavides
Universidad Surcolombiana/CENIGAA, Avenida Pastrana - Cra 1, Neiva, Huila, Colombia
E-Mail: fescobar@usco.edu.co

ABSTRACT

It is difficult to identify the mechanics of an underground reservoir and is even more difficult to identify the qualities of sites that have unusual forms. Pressure transient analysis is a tool that helps to understand what is happening inside the reservoir, understand the flow mechanisms at a macro level, and sometimes, however, they are not enough to identify flow channels generated by complex fault systems. Currently, there is not a methodology to characterize either wedge or T-shaped deposits by pressure transient testing. Then, this paper contains a careful analysis of different pressure behaviors on such systems, so numerical simulations were run for reservoirs systems considering T and wedge geometries having a well inside them in a variety of locations. The final product consists of developing an interpretation methodology using the pressure and pressure derivative log-log plot to characterize these types of reservoirs. The developed equations were succesfully tested with synthetic examples.

Keywords: reservoirs, fault, wedge, pressure, channels, TDS technique.

1. INTRODUCTION

Pressure transient tests are performed with the purpose of evaluating and determining properties of hydrocarbon-bearing formations. However, some reservoirs may have unusual shapes caused by complex faulting or deltaic channels. They possess the conditions for the formation of wedge or T-shaped systems. The complexity of the geology of such systems can be characterized by transient-pressure analysis. However, the identification and quantification of the developed systems require complex analyses, mainly, since there is no an analytical methodology for achieving the interpretation in such systems in which faults can act as leaky or sealing barriers and, depending upon their geometry and location, faulting can form elongated deposits or channels developing T or wedge shapes. Non-linear regression analysis which is by itself related to nonuniqueness is the most common way for interpretation pressure tests in the above mentioned systems.

Some studies have been conducted on the above geometrical situations. Horne, Kawaku and Temeng (1981) provided a novel analysis based upon an analytical solution to observe the pressure behavior of a well producing from a non-uniform thick stratum near to a pinch-out. Stewart and Whaballa (1980) described a new solution for compartmentalized systems based upon material balance considerations. Anisur-Rahman and Ambastha (1997) were focused on the effects of rock-fluid properties on the pressure transient in compartmentalized reservoirs. For such purpose they developed an analytical solution. They also found that certain parameters associated with the geological structure of compartments can be estimated via pressure testing. Mijinyawa and Gringarten (2008) investigated by numerical simulation four more common geometries found in complex reservoirs. They showed that all these configurations produce characteristics behaviors on well-test data which were analyzed by analogy of simpler systems. Charles, Rieke, and Purushothaman (1999) analyzed and interpreted pressure tests of two wedge off-shore reservoirs located in the south of Louisana. Anisur-Rahman, and Bentsen (2003) utilized an integrate-transformation (ITT) useful to develop new analytical solutions more powerful than the existing solutions to evaluate T and wedge shaped reservoirs.

In this paper, T and wedge geometry conditions, wedge angles and well locations were simulated to observe pressure behavior and identify unique characteristics for each system so an analytical methodology using the log-log plot of the pressure and pressure the derivative versus time is formulated and successfully tested with simulated cases.

2. MATHEMATICAL FORMULATION

2.1. Basic equations

The dimensionless time and pressure quantities used in this study are given below:

$$t_D = \frac{0.000263kt}{\phi\mu c_t r_w^2} \quad (1)$$

$$P_D = \left(\frac{kh}{141.2q\mu B}\right)\Delta P \quad (2)$$

Tiab (1993) demonstrated that the dimensionless reciprocal rate derivative during radial flow regime takes the value of 0.5,

$$[t_D * P_D']_r = 0.5 \quad (3)$$

From which the permeability is solved once the pressure derivative of Equation (2) is replaced into Equation (2), such as:

$$k = \frac{70.6 q \mu B}{h\left(t * \Delta P'\right)_r} \quad (4)$$

Where $(t*\Delta P')_r$ is the value of the pressure derivative during radial flow regime. Tiab (1993) also found an expression for the skin factor by dividing the dimensionless pressure during radial flow by Equation (4) to give;

$$s = 0.5\left\{\frac{\Delta P_r}{\left(t * \Delta P'\right)_r} - \ln\left(\frac{k t_r}{\phi \mu c_t r_w^2}\right) + 7.43\right\} \quad (5)$$

Being ΔPr the pressure drop read at any arbitrary time, tr, durinrg radial flow.

The governing pressure derivative equation during pseudosteady-state regime is given by:

$$\left[t_{DA} * P_D'\right]_p = 2\pi (t_{DA})_p \quad (6)$$

As indicated by Tiab (1994), an equation for the determination of drainage area, A, is found from the intersection point of the radial flow regime governing equation, Equation (3), and the pressure derivative equation during pseudosteady-state, Equation (6), as follows:

$$A = \frac{k t_{rpi}}{301.77 \phi \mu c_t} \quad (7)$$

Where $trpi$ is the point of intersection between the radial flow pressure derivative and the pseudosteady-state pressure derivative (extrapolated) lines.

2.2. Pressure derivative behavior for wedge-shaped reservoirs

Benavidez and Polanco (2014) performed several simulations run were performed for wedge reservoirs under variation of well location and the angle formed by the intercepting sealing faults so different empirical expressions were developed to find the angle between the intercepting faults or the distance from the well to the center of the T as will be indicated below. The different geometry combinations are given in Table-1.

2.2.1. Well located in the vortex

As described in Figure-1, the well pressure derivative trace displays initial radial flow regime and then presents a consecutive behavior as the angle changes increases from 30°, 45°, 60°, 75° y 90° so does the time to reach the boundaries; therefore, ending of radial flow time can be correlated with the angle as given in Table-2. Then, an equation for the estimation of the angle is given by:

$$\theta = 24.86956 + 0.001629975 t_{Dre} - 5.20\times10^{-6} t_{Dre}^{1.5} + 4.78\times10^{-9} t_{Dre}^{2} \quad (8)$$

Table-1. Well location and reservoir geometry.

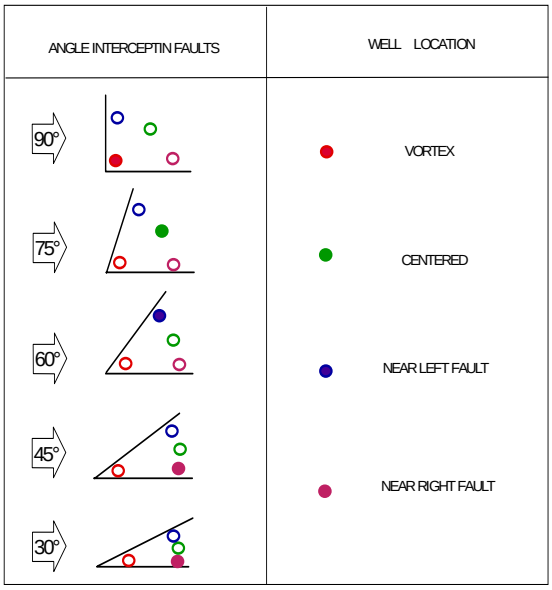

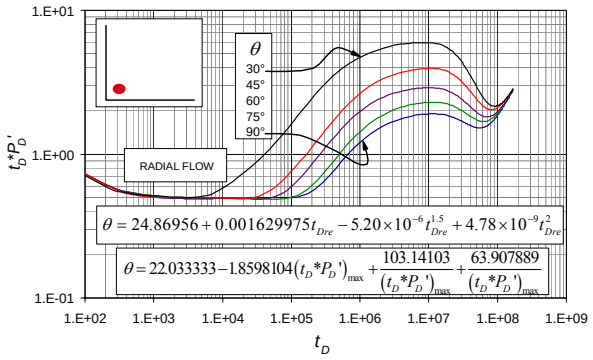

Figure-1. Pressure derivative behavior for a well located in the vortex of two intercepting faults.

Being t_{re} the time at which the radial flow regime ends and t_{Dre} is the dimensionless time for that given time.

Table-2. Values of angle and ending dimensionless time of radial flow regime for a well located in the vortex of a wedge-shaped reservoir.

t_{Dre}	θ, °
$4x10^3$	30
$2x10^4$	45
$5x10^4$	60
$1x10^5$	75
$3x10^5$	90

Another estimation of the intercepting angle is found from the maximum value of the pressure derivative before pseudosteady-state develops. These maximum points against angle are given in Table-3 from which the following expression was obtained:

$$\theta = 22.033333 - \frac{0.0131715kh(t*\Delta P')_{max}}{q\mu B} + \frac{14563.5134q\mu B}{kh(t*\Delta P')_{max}} + \frac{(q\mu B)^2}{311.97\left[kh(t*\Delta P')_{max}\right]^2} \quad (9)$$

Table-3. Values of angle and maximum dimensionless pressure derivative values for a well located in the vortex of a wedge-shaped reservoir.

$(t_D*P_D')_{max}$	$(t_D*P_D')_{min}$	θ, °
5.97	2.15	30
3.94	2.04	45
2.98	1.88	60
2.29	1.68	75
1.91	1.52	90

The minimum value of the pressure derivative that shows up just before the development of the pseudosteady-state regime was also correlated to find the intersecting angle and their values are reported in Table-3. The resulting correlation is given by:

$$\theta = 288.55277 - 159.05376(t*P_D')_{min}^2 + 41.012164(t*P_D')_{min}^4 - 4.0464308(t*P_D')_{min}^6 \quad (10)$$

2.2.2. Well located near the right fault

It is observed in Figure-2 that once the near fault is felt a transition period develops and a hemi-radial flow regime shows up and vanishes once the other fault is reached by the disturbance. Before the pseudosteady-state, a maximum shows up as the intercepting angle is smaller than 60°. For this case, the characteristic point used was the dimensionless time for the transient wave to reach the far fault which values for each study angle are given in Table-4.

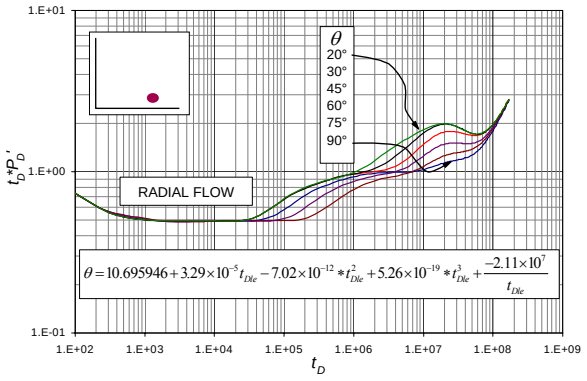

Figure-2. Pressure derivative behavior for a well located at the right fault of the vortex.

Equation (11) was obtained for estimating the intersecting angle for this case.

$$\theta = 10.695946 + 3.29\times10^{-5}t_{Dle} - 7.02\times10^{-12}t_{Dle}^2 + 5.26\times10^{-19}t_{Dle}^3 - \frac{2.11\times10^7}{t_{Dle}} \quad (11)$$

2.2.3. Well located at the left fault

This case which dimensionless pressure derivative reported in Figure-3 is very similar to the former one which means that Equation (11) can be applied. However, in this case the ending time of the radial flow regime against the angle, see Table-5, was used to develop the following expression:

$$\theta = \frac{27.804247 + 3.92\times10^{-9}t_{Dre}^2}{1 + 3.8\times10^{-11}t_{Dre}^2} \quad (12)$$

Table-4. Values of angle and dimensionless inflection time after reaching the second fault for a well located in the vortex of a wedge-shaped reservoir.

t_{Dle}	θ, °
$1.11\text{x}10^6$	20
$1.4\text{x}10^6$	30
$2.22\text{x}10^6$	45
$4.4\text{x}10^6$	60
$7.03\text{x}10^6$	75
$7.91\text{x}10^6$	90

Table-5. Values of angle and ending dimensionless time of radial flow regime for a well flow a well located near the left fault of a wedge-shaped reservoir.

t_{Dre}	θ, °
$2.8\text{x}10^4$	30
$8.83\text{x}10^4$	45
$1.4\text{x}10^5$	60
$3.52\text{x}10^5$	90

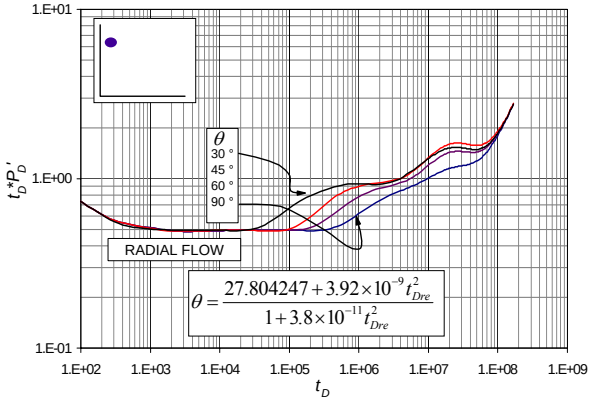

Figure-3. Pressure derivative behavior for a well located at the left fault of the vortex.

2.2.4. Well located at the center

The pressure derivative behavior of a well located in the middle point of two intersecting faults is given in Figure-4 for angles of 20°, 30°, 45°, 60°, 75° and 90°. As the intersecting angle increases the time required to finish the radial flow regime also increases. See also Table-6. Pseudosteady state develops once all the reservoir boundaries are reached.

Table-6. Values of angle and ending of radial flow for a well located in the center of two sealing faults in a wedge-shaped reservoir.

t_{Dre}	θ, °
2.79x10^5	20
5.57x10^5	30
8.83x10^5	45
1.11x10^6	60
1.2x10^6	75
1.4x10^6	90

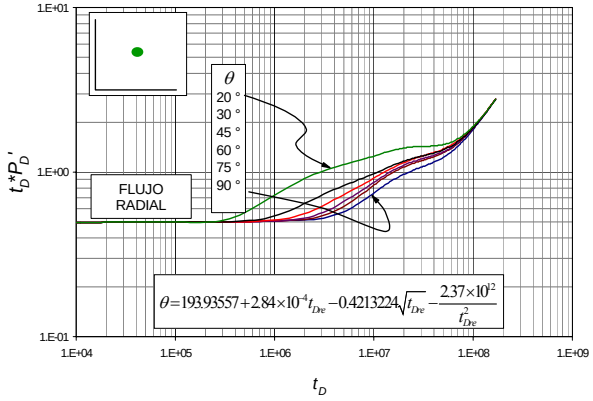

Figure-4. Pressure derivative behavior for a well located at the center of two sealing faults.

Equation (13) was obtained using the data from Table-5.

$$\theta = 193.93557 + 2.84\times10^{-4} t_{Dre} - 0.4213224\sqrt{t_{Dre}} - \frac{2.37\times10^{12}}{t_{Dre}^2} \quad (13)$$

2.3. Pressure derivative behavior for T-shaped reservoirs

For this type of systems, simulations were performed for different well locations inside the system according to labels A through E as depicted in Figure-4. The pressure derivative behavior for each case is reported in Figure-5. Notice that the closer to the center of the T, the longer the duration of the radial flow. After the radial flow vanishes, Case A presents a combination of two perpendicular linear flow regimes while case E has an initial predominant linear flow that later combines with another radial flow coming from the lower part of the T. As a final behavior, pseudosteady-state is developed.

Since a characteristic pattern was not observed, the next step was to study the second dimensionless pressure derivative behavior. Case E was taken out of the analysis since is located too close to the west boundary, then, its behavior does not follow an established pattern as given in Figure-6, from which data reported in Table-7 was read.

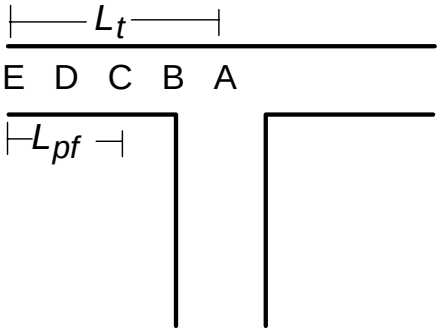

Figure-4. Well location inside the T-shaped reservoir.

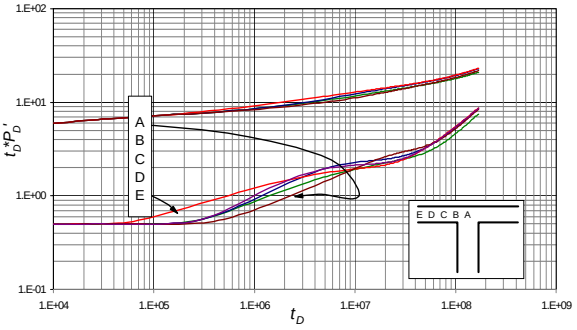

Figure-5. Pressure derivative behavior for a well located along a T-shaped reservoir.

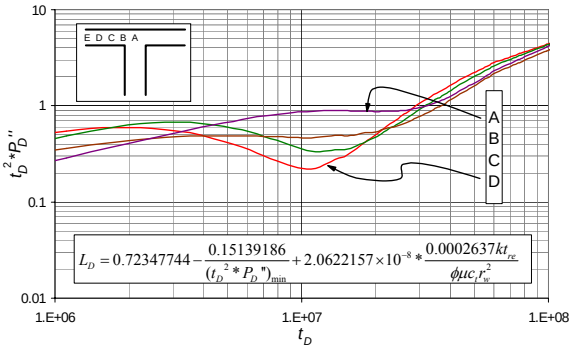

Figure-6. Second pressure derivative behavior for a well located along a T-shaped reservoir.

A dimensionless distance was defined as the ratio between the distance from the west or east boundary to the center, thus;

$$L_D = \frac{L_{pf}}{L_t} \quad (14)$$

Information from Table-7 led to develop an expression for the estimation of the distance from the well to one of the boundaries along the upper region of the T, see Figure-4, as follows:

$$L_D = 0.72347744 - \frac{21.3774 q \mu B}{kh(t^2 * \Delta P'')_{\min}} + 5.42363 \times 10^{-12} \frac{k t_{re}}{\phi \mu c_t r_w^2} \quad (15)$$

Table-7. Coordinates of the minimum value of the second pressure derivative for each dimensionless length.

$(t_D*P_D'')_{min}$	$(t_D)_{min}$	L_D
0.868894	22000000	1
0.464527	15800000	0.75
0.334065	11400000	0.5
0.219073	10500000	0.25

3. EXAMPLES

Three synthetic examples were run with the information given below:

$\phi = 20\%$ $r_w = 0.5$ ft q =500 STB/D
$h = 100$ ft $B_o = 1.15$ bls/STB $\mu = 5$ cp
$c_t = 4\text{x}10^{-6}$ psi^{-1} A = 990855995.8 ft^2

3.1. Example-1

Pressure and pressure derivative against time data are reported in Figure-7 for the case of a well located near the vortex of two sealing faults. It is required to estimate permeability, skin factor, drainage area and the angle formed between the two faults.

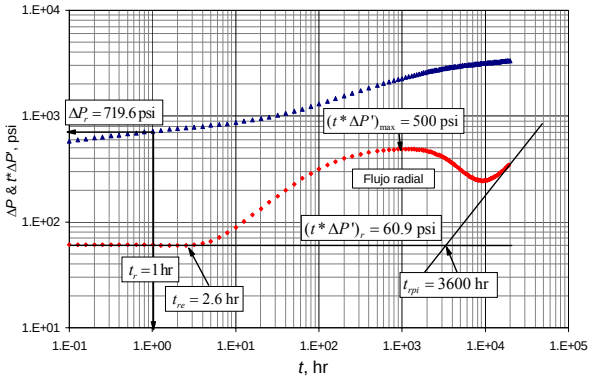

Figure-7. Log-log plot of pressure and pressure derivative vs. time for example-1.

Solution

The following information was read from Figure-7:

$t_r = 1$ hr $\Delta P_r =$ 719.6 psi
$(t*\Delta P')\,r = 60.9$ psi $t_{re} = 2.6$ hr
$(t*\Delta P')_{max} = 500$ psi

Permeability and skin factor are estimated with Equations (4) and (5), respectively, thus:

$$k = \frac{(70.6)(500)(5)(1.15)}{(100)(60.9)} = 33.3 \text{ md}$$

$$s = 0.5\left\{19.6 - \ln\left(\frac{(33.3)(1)}{(0.2)(5)(4\times10^{-6})(0.5^2)}\right) + 7.43\right\} = 0.9$$

Drainage area is found using Equation (7),

$$A = \frac{(33.3)(10100)}{301.77(0.2)(5)(4\times10^{-6})} = 99314047.1 \text{ ft}^2$$

Equation (1) allows translating the actual time to dimensionless time,

$$t_{Dre} = \frac{(0.0002637)(33.3)(2.6)}{(0.2)(1.15)(4\times10^{-6})(0.5^2)} = 23000$$

The intercepting angle is found after replacing he above value into Equation (8),

$$\theta = 24.86956 + 0.001629975(23000) - 5.20\times10^{-6}(23000)^{1.5} + 4.78\times10^{-9}(23000)^2 = 46.75°$$

The angle of intersection can be verified using the maximum point of the pressure derivative in Equation (9), thus,

$$\theta = 22.033333 - \frac{0.0131715(33.3)(100)(500)}{(500)(5)(1.15)} + \frac{14563.5134(500)(5)(1.15)}{(33.3)(100)(500)} + \frac{9023.7939(500)(5)(1.15)}{(33.3)(100)(500)} = 43.4°$$

3.2. Example-2

The same input data for the former example was applied for a wedge-shaped reservoir with the well centered. The input intercepting angle was 70°. Pressure derivative data is reported in Figure-8. It required finding the intersecting angle.

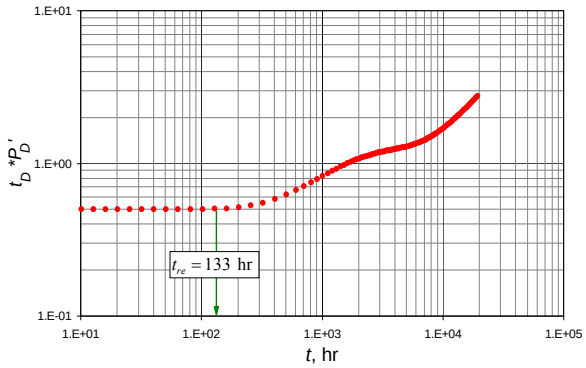

Figure-8. Log-log plot of pressure derivative vs. time for example-2.

Solution

A value of t_{re} of 133 hr was read from Figure-8 which translates into a dimensionless time of 1.16×10^6. This allows finding an intersection angle of 67° by means of Equation (13).

3.3. Example-3

A pressure test of T-shape reservoir was simulated using the data mentioned at the beginning of the examples. The well is located in the B position given in Figure-4 and the total length from the well to the middle position (point A in Figure-4) was 2600 ft. Data of the pressure derivative and second pressure derivative against time are reported in Figure-9. It is required to find the length of the B position.

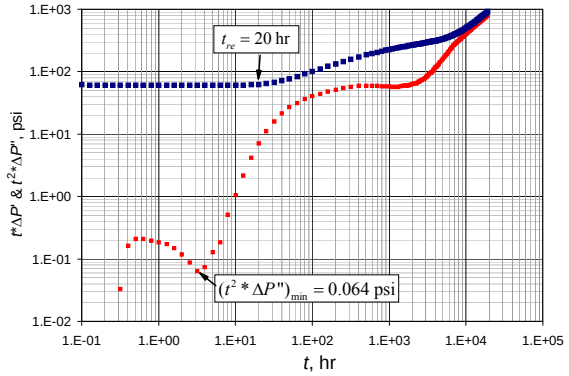

Figure-9. Log-log plot of pressure derivative and second pressure derivative vs. time for example-3.

Solution

A value of t_{re} of 20 hr and a minimum second derivative of 63 psi were read from Figure-9. The corresponding dimensionless values found with Equation 1 and the second derivative of Equation 1 result into:

$t_{Dre} = 176000$
$(t_D^2 * P_D'')_{min} = 0.513$

Use of Equation (15) leads to find a dimensionless length of 0.44 which multiplied by 2600 translates into 1152.12 ft.

4. COMMENT ON THE RESULTS

The values of intersecting angles and distance from boundary to well were in close agreement with the values used for the simulation which verify the validity of the given correlations.

5. CONCLUSIONES AND RECOMMENDATIONS

Pressure behavior was studied for a well located inside both wedge-shape (simulated with intersecting sealing faults) and T-Shaped reservoirs which led to the development of new equations to find the intersecting angle and the distance from the boundary to the well. The developed expressions were successfully tested with synthetic examples.

ACKNOWLEDGEMENTS

The authors gratefully thank the Most Holy Trinity and the Virgin Mary mother of God for all the blessing received during their lives.

The author also thanks Universidad Surcolombiana for providing financial support for the complement of this study.

Nomenclature

A	Draining area, ft^2
B	Oil volume factor, rb/STB
c_t	Compressibility, 1/psi
h	Formation thickness, ft
k	Formation compressibility, md
P	Pressure, psi
P_{wf}	Well-flowing pressure, psi
q	Flow rate, STB/D
r_e	Drainage radius, ft
r_w	Wellbore radius, ft
s	Skin factor
t	Test time, hr
$(t*\Delta P')$	Pressure derivative, psi
$(t^2*\Delta P'')$	Second pressure derivative, psi
(t_D*P_D')	Dimensionless pressure derivative
$(t_D^2*P_D'')$	Dimensionless second pressure derivative
L_{pf}	Distance from boundary to center, ft
L_t	Lenght from boundary to middle of

Greek

Δ	Change
ϕ	Porosity, fracction
μ	Viscosity, cp

Suffixes

D	Dimensionless
le	inflection time after reaching the second fault
max	Maximum
r	Radial
re	End of radial flow
rpi	Intersect of radial-pseudosteady state lines
w	well
t	tiempo
p	Pseudosteady-state

REFERENCES

Anisur-Rahman A. and Bentsen B. 2003. New Analytical Solutions for Predicting Pressure Distribution and Transient Behavior in Wedges and Truncated Wedges. Paper SPE 71585, SPE Journal, September.

Benavides W. and Polanco M. P. 2014. Interpretación de Pruebas de Presión en Yacimientos Acuñados y en Forma de T. B.Sc. Thesis. Universidad Surcolombiana, February.

Charles D. D., Rieke H. H. and Purushothaman R. 1999. Well Test Characterization of Wedge-Shaped, Faulted Reservoirs. Paper SPE 56685. October.

Mijinyawa A. and Gringarten A. C. 2008. Influence of geological features and well test behavior. Paper SPE 113877, Roma, Italia junio de.

Roland N., Horne and Kawaku O. and Temeng 1981. Recognition and Location of Pinchout Boundaries by Pressure Transient Analysis. Paper SPE 9905, March.

Stewart G. and Whaballa A. E. 1980. Pressure Behavior of Compartmentalized Reservoirs. Paper SPE 19779, October.

Tiab D. 1993. Analysis of Pressure and Pressure Derivative without Type-Curve Matching: 1- Skin and Wellbore Storage. Journal of Petroleum Science and Engineering. 12: 171-181.

Tiab D. 1994. Analysis of Pressure and Pressure Derivative without Type Curve Matching: Vertically Fractured Wells in Closed Systems. Journal of Petroleum Science and Engineering. 11: 323-333.